

Matrix Madness and Complex Confusion...

A Review of Complex Modes from Multiple Viewpoints

George Fox Lang, Associate Editor

Complex Modes is one of those topics that every vibration practitioner understands – just not fully. We all “know” that complex modes exhibit two shape functions that vibrate at a single frequency in phase quadrature. Experimentalists recognize complex modes from the “galloping nodes” in an animated display. Analysts understand them as result of the “non-proportional” distribution of damping. Most of us have found some aspect of the complex mode phenomenon, its analysis or measurement just a little mysterious.

I will confess burning a disproportionate number of the many calories I have consumed in pursuit of a strong “gut feel” for complex modes. This article is intended as a brief reference document for anyone suffering from the same hunger. When I first entered professional engineering practice in 1966, vibration analysts and test practitioners were focused on finding a structure’s *normal modes*. Our analytic tools were dominated by matrix methods applied to “lumped mass” models. Testing techniques employed slowly swept sine excitation and tracking filter analysis. No one bandied the term “complex mode” about, animated mode shape displays were eons in the future (we hand plotted our mode shapes) and mode shapes with nodal points that “travel” would have been viewed as the result of experimental or numerical error.

About a decade later, fast Fourier transform (FFT) signal analysis, impulse testing and (later) *complex modes* dominated everyone’s interest and lexicon. Around this time, interest in developing new structural modeling methods evaporated in favor of refining and extending *finite-element* (FE) analysis, the new technical darling fed by ever-increasing computer power and the disbursed availability of such power. Complex modes came to become a really “big deal” in experimental practice in the mid ’70s. They have yet to be as thoroughly accepted by the analytic modeling community. This probably has much to do with the focus (or lack of focus) of today’s FE marketing executives. I believe it will be beneficial to practitioners old and new to review the evolution of complex-mode modeling and test analysis.

On the Analytic Side – Normal Modes

Much of my early business life was spent in the study of systems described by “lumped mass” models. In that era, matrix notation was the modern language of vibration analysis. I learned to speak *matrix* (possibly an Australian dialect in a heavy Scottish accent with strong Brooklyn overtones) fluently while working for Sikorsky Aircraft Corporation. As a lowly BSME “fresh-out” surrounded by seasoned PhDs, it was incumbent upon me to catch up quickly to avoid being tossed all of the “dog work.” My coworkers became good friends and excellent mentors. The majority of problems we studied were eventually described by a system of second-order, linear differential, forced-motion equations of the form:

$$[M]\{\ddot{x}\} + [C]\{\dot{x}\} + [K]\{x\} = \{F\} \quad (1)$$

By far the most difficult task was solving such equations for natural frequencies and mode shapes. In the mid ’60s, it was common practice to ignore damping altogether when solving such eigenvalue/eigenvector problems. We often tried to pass off the notion of ignoring damping as seeking a conservative solution, since any damping found in the actual structure would help diminish undesired vibration. In any event, many problems in the form of Equation 2 were solved for undamped natural frequencies and normal-mode shapes.

$$[M]\{\ddot{x}\} + [K]\{x\} = \{F\} \quad (2)$$

This was accomplished by applying the following three constraints to Equation 2:

- (a) $\{F\} = \{0\}$
- (b) $\{x\} = \{\phi\} \cos(\omega t)$
- (c) $\{\ddot{x}\} = -\omega^2 \{\phi\} \cos(\omega t)$

This simplified the problem to the form:

$$[K]\{\phi\} = \omega^2 [M]\{\phi\} \quad (3)$$

Inverting the stiffness matrix, K , allowed the equations to be placed in the standard “ λ -matrix” or eigenvalue/eigenvector format (Eq. 4). The scalar, λ , was termed an eigenvalue, while the vector, $\{\phi\}$, was called an eigenvector. $[K^{-1}]$ was called an *influence coefficient matrix* and $[D]$ the *dynamic matrix*. Influence coefficients were often actually measured in the laboratory by applying known forces and measuring the resulting displacement patterns. This was practical; directly measuring a stiffness matrix, by applying known displacement patterns and measuring the forces necessary to maintain them, was not.

$$\frac{1}{\omega^2} \{\phi\} = \lambda \{\phi\} = [K^{-1}][M]\{\phi\} = [K^{-1}M]\{\phi\} = [D]\{\phi\} \quad (4)$$

Eigen is from the German for *particular*. To appreciate the particularity sought, consider what Equation 4 says geometrically. The left side of Eq. 4 multiplies a vector by a scalar. This operation merely extends or contracts the vector length; it does not change the vector’s orientation. In contrast, the right side of Eq. 4 multiplies the same vector by a matrix. Such multiplication potentially changes both the length and direction of the vector. Therefore, an eigenvector, $\{\phi_n\}$, of these equations is a vector that does not change its direction when premultiplied by $[D]$. However such multiplication extends the vector’s length by a factor of λ_n . In general, a system of N equations will have N unique eigenvalue/eigenvector pairs. Each eigenvalue is the reciprocal of a squared natural frequency in radians/second. Each corresponding eigenvector models the associated mode shape.

$$\{x\} = [\{\phi_1\}\{\phi_2\}\dots\{\phi_n\}\dots\{\phi_N\}]\{q\} = [\phi]\{q\} \quad (5)$$

The N mode shapes may be assembled to form a coordinate transform matrix by “stacking” the found eigenvectors side-by-side as shown in Eq. 5. This transformation describes any arbitrarily deformed shape of the structure as a linear combination of the mode shapes. Substituting Eq. 5 in Eq. 3 results in Eq. 6a:

$$[M][\phi]\{\ddot{q}\} + [K][\phi]\{q\} = \{F\} \quad (6a)$$

Premultiplying Eq. 6a by the transpose of the transformation completes a *similarity transformation*, with the result shown in Eq. 6b. The resulting diagonal matrices are referred to as the *generalized mass* and *generalized stiffness* matrices (sometimes termed *modal mass* and *modal stiffness*). The vector, $\{Q\}$, is called a *generalized force*. The $\{q\}$ vector is often termed a *modal participation* vector:

$$[\phi^T][M][\phi]\{\ddot{q}\} + [\phi^T][K][\phi]\{q\} = [\phi^T]\{F\} = \{Q\} \quad (6b)$$

The similarity transformation of Equations 6a and 6b disclose an important property of the modal vectors: they exhibit *generalized orthogonality* with respect to the mass and stiffness matrices. That is, they diagonalize both matrices, thereby uncoupling all N equations from one another:

$$[M_n]\{\ddot{q}\} + [\omega^2 M_n]\{q\} = \{Q\} \quad (7)$$

In general, each of the N diagonal M_n elements is different. The actual numerical value of each M_n is determined by how the $\{\phi_n\}$ vectors were *normalized*. Scaling methods, such as setting the largest vector element or the top-most element or the vector length to 1 will each result in a different set of M_n values. One very at-

tractive option is to choose the length of the $\{\phi_n\}$ vectors so that the generalized mass matrix becomes an identity matrix. Modal vectors normalized in this manner are said to be *orthonormalized*. The corresponding generalized stiffness matrix then contains the corresponding squared circular natural frequencies on the diagonal and zeros everywhere else.

Note that the generalized orthogonality is guaranteed because of known mathematical properties of the $[M]$ and $[K]$ matrices. In specific, both are *symmetrical*, reflecting reciprocity or *structural isotropy*. Further, the $[K]$ matrix is known to be *positive-definite*, indicating that the modeled structure is determinate; that is, it won't topple over. Note also that the solution vectors do not generally exhibit *ordinary orthogonality* to one another. That is:

$$\{\phi\}^T [\phi] \neq [I] \quad (8)$$

Normal or real modes can uncouple the damped equations of motion (Eq. 1) but only in a very limited case. Such damped structural models uncoupled by normal modes are said to be *proportionately damped*, meaning the damping matrix, $[C]$, can be expressed as a linear combination of the mass and stiffness matrices as asserted by Equation 9a:

$$[C] = \alpha[M] + \beta[K] \quad (9a)$$

So, when the damping matrix of a proportionately damped system is subjected to similarity transformation using the normal modes, $[\phi]$, a diagonal *generalized* or *modal damping* matrix results, as asserted by Equation 9b. Since proportionality is never guaranteed, this is not a general solution to Equation 1:

$$[\phi^T][C][\phi] = \begin{bmatrix} \ddots & & & \\ & \alpha M_n + \beta \omega_n^2 M_n & & \\ & & \ddots & \\ & & & \ddots \end{bmatrix} = \begin{bmatrix} \ddots & & & \\ & 2\xi_n \omega_n M_n & & \\ & & \ddots & \\ & & & \ddots \end{bmatrix} = \begin{bmatrix} \ddots & & & \\ & C_n & & \\ & & \ddots & \\ & & & \ddots \end{bmatrix} \quad (9b)$$

On the Analytic Side – Complex Modes

A general solution to the damped vibration problem is possible, but it requires recasting the equations in a different manner. First, the velocities at each degree of freedom (DOF) are treated as a separate, state-variable vector, $\{v\}$. Second, differentiation is restricted to *first order* only. This amounts to changing Eq. 1 to Eq. 10a. Third, a second equation (Eq. 10b) reflecting a momentum balance between $\{\dot{x}\}$ and $\{v\}$, is solved simultaneously:

$$[M]\{\dot{v}\} + [C]\{\dot{x}\} + [K]\{x\} = \{F\} \quad (10a)$$

$$[M]\{\dot{x}\} - [M]\{v\} = \{0\} \quad (10b)$$

The combined equations to be simultaneously solved are presented in Eq. 11. In essence, we have traded solving N second-order differential equations for $2N$ first-order equations. The combined matrices are each of size $2N \times 2N$.

$$\begin{bmatrix} 0 & M \\ M & C \end{bmatrix} \begin{Bmatrix} \dot{v} \\ \dot{x} \end{Bmatrix} + \begin{bmatrix} -M & 0 \\ 0 & K \end{bmatrix} \begin{Bmatrix} v \\ x \end{Bmatrix} = \begin{Bmatrix} 0 \\ F \end{Bmatrix} \quad (11)$$

Equation 11 is solved for frequency, damping and (complex) mode shape by assuming the external forces to be zero (a), and defining the state variable vectors in terms of complex exponential functions of time (b) and (c):

$$\begin{aligned} \text{(a)} \quad & \begin{Bmatrix} 0 \\ F \end{Bmatrix} = \begin{Bmatrix} 0 \\ 0 \end{Bmatrix} \\ \text{(b)} \quad & \begin{Bmatrix} v \\ x \end{Bmatrix} = \begin{Bmatrix} P\psi \\ \psi \end{Bmatrix} e^{pt} \\ \text{(c)} \quad & \begin{Bmatrix} \dot{v} \\ \dot{x} \end{Bmatrix} = p \begin{Bmatrix} P\psi \\ \psi \end{Bmatrix} e^{pt} \end{aligned}$$

Equation 12a presents the result of applying these three actions to Eq. 11:

$$p \begin{bmatrix} 0 & M \\ M & C \end{bmatrix} \begin{Bmatrix} P\psi \\ \psi \end{Bmatrix} = - \begin{bmatrix} -M & 0 \\ 0 & K \end{bmatrix} \begin{Bmatrix} P\psi \\ \psi \end{Bmatrix} \quad (12a)$$

Premultiplying Eq. 12a by the inverse of the right-hand matrix and rearranging terms results in Eq. 12b, which is clearly of the same $\lambda\{\phi\} = [D]\{\phi\}$ form as Eq. 4. So, solution by the same general mathematical methods is possible:

$$\frac{1}{p} \begin{Bmatrix} P\psi \\ \psi \end{Bmatrix} = \begin{bmatrix} 0 & I \\ -K^{-1}M & -K^{-1}C \end{bmatrix} \begin{Bmatrix} P\psi \\ \psi \end{Bmatrix} \quad (12b)$$

Note that all of the matrix elements in Eq. 12b are real valued. Only the eigenvector elements and the eigenvalue are complex quantities.

Analytically, Solving for Frequency, Damping and Shape

I have discussed the formulation of characteristic real-mode (Eq. 4) and complex-mode (Eq. 12b) eigenvalue/eigenvector equations, and the properties of the resulting frequency values and shape vectors. But I have not discussed the methods of solving for the eigenproperties; this choice was deliberate. There are many competing algorithms available to solve such problems, and it is not my intent to champion any one of them. However, some general comments regarding solution methods seem appropriate.

$$[[D] - \lambda[I]] = 0 \quad (13)$$

The eigenvalues of $\lambda\{\phi\} = [D]\{\phi\}$ are the roots of the characteristic polynomial that results from evaluating the determinant (Eq. 13), where $[I]$ denotes the identity matrix. For an $N \times N$ real-mode formulation, N distinct real eigenvalues result. For a complex-mode formulation, the same $[M]$ and $[K]$ matrices lead to a $[D]$ matrix of $2N \times 2N$ and N pairs of conjugate complex eigenvalues.

$$[[D] - \lambda[I]]\{\phi\} = \{0\} \quad (14)$$

Once the eigenvalues are known, the corresponding eigenvectors may be evaluated one at a time. This is accomplished by substituting one of the known λ (say λ_n) into Eq. 14, assuming the value for one element (say $\phi_n = 1$) of the $\{\phi_n\}$ vector and algebraically solving for the remaining $N-1$ elements of $\{\phi_n\}$. This process is repeated until all of the eigenvectors have been obtained.

Since solving for the roots of a high-order polynomial is a daunting numeric task, alternative algorithms have evolved over the years. One of the most popular and successful methods is called *matrix iteration*. It uses an old standard in higher mathematics: guessing the answer. Start by guessing a trial vector, $\{T_n^k\}$, to approximate sought modal vector, $\{\phi_n\}$. Normalize $\{T_n^k\}$ to become $\{\bar{T}_n^k\}$ by dividing all of its elements by the largest element in the vector. Recursively execute Equation 15 until the trial vector and its normalizing eigenvalue stabilize. Retain these stabilized values as $\{\phi_n\}$ and λ_n respectively.

$$[D]\{\bar{T}_n^k\} = \{T_n^{k+1}\} = \lambda_n^{k+1} \{\bar{T}_n^{k+1}\} \quad (15)$$

Iteration of the $[D]$ matrix will always converge on the largest *eigenvalue*, regardless of the vector shape chosen as the initial guess. Since (in the real mode case), $\lambda_n = 1 / \omega_n^2$, this guarantees that the lowest frequency or first mode will be converged upon. To converge upon higher modes, the orthogonality properties demonstrated in Eq. 7 are employed. After the first mode is known, the elements of the $\{\phi_1\}$ eigenvector and elements of the original mass matrix, $[M]$, are combined to form a *sweeping matrix*, $[S_1]$. The recursion equation is modified to Equation 16, and the second mode is sought:

$$[D][S_1]\{\bar{T}_2^k\} = \{T_2^{k+1}\} = \lambda_2^{k+1} \{\bar{T}_2^{k+1}\} \quad (16)$$

The $[S_1]$ matrix causes each trial vector to be *purified* of $\{\phi_1\}$ content. That is, vector content in $\{T_n\}$ proportional to $\{\phi_1\}$ is effectively subtracted out, forcing the iteration to converge on the second mode. After each successful convergence to a mode, a new $[S_n]$ matrix is developed using elements of all found eigenvectors and the iteration is implemented again to obtain $\{\phi_{n+1}\}$.

For reference, it is also possible to recast the recursion in terms of the inverse dynamic matrix, $[D^{-1}] = [M^{-1}][K]$. In this case, the

recursion will converge to the smallest eigenvalue or highest frequency. This can be of value, since the errors in frequency and shape increase with each mode found.

Experimental Side – Normal Modes

Experimental modal analysis is very much about curve fitting measurements. In particular, measured motion/force *frequency response functions* (FRFs) are matched to theoretical FRFs derived from a real or complex-mode model. The desired resonance frequencies, damping and mode shapes are computed from the results of hundreds of curve fits. There are dozens of modern curve fitters applied to this problem, and each has its champion. It is not my purpose to determine the best of these; I just want to explain the parameters of the theoretical models matched by proper curve fitting.

For an undamped structure or one with proportional damping, performing modal vector similarity transformation on the Equation 1 results in N uncoupled equations in the form of Equation 17a. The resulting generalized mass, damping and stiffness are all diagonal matrices:

$$\begin{aligned} & [\phi^T][M][\phi]\{\ddot{q}\} + [\phi^T][C][\phi]\{\dot{q}\} + [\phi^T][K][\phi]\{q\} = \\ & [M_n]\{\ddot{q}\} + [2\xi_n\omega_n M_n]\{\dot{q}\} + [\omega_n^2 M_n]\{q\} = [\phi^T]\{F\} = \{Q\} \end{aligned} \quad (17a)$$

Assuming all initial conditions are zero and applying the *LaPlace Transform* to these results produces:

$$[M_n S^2 + 2\xi_n\omega_n M_n S + \omega_n^2 M_n]\{q\} = \{Q\} \quad (17b)$$

Since the matrix in Equation 17b is diagonal, inverting it is trivial, and we can state:

$$\{q\} = \left[\frac{1}{M_n S^2 + 2\xi_n\omega_n M_n S + \omega_n^2 M_n} \right] \{Q\} \quad (18)$$

If a single force is applied to the structure (say at DOF, x_a), the generalized force vector, $\{Q\}$, can be written as Equation 19. This equation shows that exciting a single degree of freedom excites all N modes in the structural model simultaneously:

$$\{Q\} = \begin{Bmatrix} Q_1 \\ \vdots \\ Q_N \end{Bmatrix} = [\phi^T]\{F\} = \begin{Bmatrix} \phi_{a,1} \\ \vdots \\ \phi_{a,N} \end{Bmatrix} F_a \quad (19)$$

The resulting motion at a single DOF (say, x_b) is contained in the more general result (Eq. 5). This allows us to write Equation 20, and note that x_b contains contributions from all N modes.

$$x_b = [\phi_{b,1} \dots \phi_{b,N}] \begin{Bmatrix} q_1 \\ \vdots \\ q_N \end{Bmatrix} \quad (20)$$

Thus the FRF, $H_{a,b}(S)$, may be stated as:

$$H_{a,b}(S) = [\phi_{b,1} \dots \phi_{b,N}] \left[\frac{1}{M_n S^2 + 2\xi_n\omega_n M_n S + \omega_n^2 M_n} \right] \begin{Bmatrix} \phi_{a,1} \\ \vdots \\ \phi_{a,N} \end{Bmatrix} = \sum_{n=1}^N \frac{\phi_{a,n}\phi_{b,n}}{M_n(S^2 + 2\xi_n\omega_n S + \omega_n^2)} \quad (21)$$

Experimental Side – Complex Modes

A similar derivation for $H_{a,b}(S)$ may be made from the complex-mode formulation of Equation 11. Note that for a system with N degrees of freedom, the solution to Equations 11 is comprised of $2N$ eigenvalues and eigenvectors. Each eigenvalue is associated with a complex vector of length $2N$. These $2N$ roots and $2N$ vectors are actually found in complex-conjugate pairs. This four-fold increase in information is at first confusing, until we remember that each complex modal vector reflects N velocity and N displacement DOFs. Since the original physical v_i and x_i variables are real-valued functions of time, a complex vector *and its conjugate* are simultaneously required to reconstruct them.

The complex-mode solution vectors may be assembled into a transformation matrix as was done in Equation 5 for the real mode formulation. Specifically:

$$\begin{Bmatrix} v_1 \\ \vdots \\ v_N \\ x_1 \\ \vdots \\ x_N \end{Bmatrix} = \begin{bmatrix} p_1\psi_{1,1} & \dots & p_N\psi_{1,N} & p_1^*\psi_{1,1}^* & \dots & p_N^*\psi_{1,N}^* \\ \vdots & & \vdots & \vdots & & \vdots \\ p_1\psi_{N,1} & \dots & p_N\psi_{N,N} & p_1^*\psi_{N,1}^* & \dots & p_N^*\psi_{N,N}^* \\ \psi_{1,1} & \dots & \psi_{1,N} & \psi_{1,1}^* & \dots & \psi_{1,N}^* \\ \vdots & & \vdots & \vdots & & \vdots \\ \psi_{N,N} & \dots & \psi_{N,N} & \psi_{N,1}^* & \dots & \psi_{N,N}^* \end{bmatrix} \begin{Bmatrix} q_1 \\ \vdots \\ q_N \\ q_1^* \\ \vdots \\ q_N^* \end{Bmatrix} \quad (22)$$

Applying Eq. 22 to Eq. 11 as a similarity transformation results in the uncoupled equations abbreviated here:

$$\begin{bmatrix} M_n & 0 \\ 0 & M_n \end{bmatrix} \begin{Bmatrix} \dot{q} \\ \dot{q}^* \end{Bmatrix} + \begin{bmatrix} -M_n p_n & 0 \\ 0 & -M_n p_n^* \end{bmatrix} \begin{Bmatrix} q \\ q^* \end{Bmatrix} = \begin{Bmatrix} Q \\ Q^* \end{Bmatrix} \quad (23)$$

Applying the LaPlace transform with all initial conditions equal to zero results in:

$$\begin{bmatrix} M_n(S - p_n) & 0 \\ 0 & M_n(S - p_n^*) \end{bmatrix} \begin{Bmatrix} q \\ q^* \end{Bmatrix} = \begin{Bmatrix} Q \\ Q^* \end{Bmatrix} \quad (24)$$

The matrix inversion of Eq. 25 is trivial, since all the off-diagonal elements are equal to zero:

$$\begin{bmatrix} \frac{1}{M_n(S - p_n)} & 0 \\ 0 & \frac{1}{M_n(S - p_n^*)} \end{bmatrix} \begin{Bmatrix} Q \\ Q^* \end{Bmatrix} = \begin{Bmatrix} q \\ q^* \end{Bmatrix} \quad (25)$$

Applying a single force to a DOF produces a generalized force that excites all of the modes (and their conjugates) in accordance with:

$$\begin{Bmatrix} Q \\ Q^* \end{Bmatrix} = \begin{Bmatrix} Q_1 \\ \vdots \\ Q_N \\ Q_1^* \\ \vdots \\ Q_N^* \end{Bmatrix} = \begin{Bmatrix} \psi_{a,1} \\ \vdots \\ \psi_{a,N} \\ \psi_{a,1}^* \\ \vdots \\ \psi_{a,N}^* \end{Bmatrix} F_a \quad (26)$$

The response displacement at DOF **b** is given by:

$$x_b = [\psi_{b,1} \dots \psi_{b,N} \quad \psi_{b,1}^* \dots \psi_{b,N}^*] \begin{Bmatrix} q_1 \\ \vdots \\ q_N \\ q_1^* \\ \vdots \\ q_N^* \end{Bmatrix} \quad (27)$$

Combining Equations 25-27 provides the displacement/force FRF between DOFs **a** and **b**:

$$[\psi_{b,1} \dots \psi_{b,N} \quad \psi_{b,1}^* \dots \psi_{b,N}^*] \begin{bmatrix} \frac{1}{M_n(S - p_n)} & 0 \\ 0 & \frac{1}{M_n(S - p_n^*)} \end{bmatrix} \begin{Bmatrix} \psi_{a,1} \\ \vdots \\ \psi_{a,N} \\ \psi_{a,1}^* \\ \vdots \\ \psi_{a,N}^* \end{Bmatrix} = \quad (28)$$

$$\sum_{n=1}^N \frac{\psi_{a,n}\psi_{b,n}}{M_n(S - p_n)} + \frac{\psi_{a,n}^*\psi_{b,n}^*}{M_n(S - p_n^*)} = H_{a,b}(S)$$

Substitute the following six definitions for the complex variables in Eq. 28:

- (a) $p_n = -\sigma_n + j\Omega_n$
- (b) $p_n^* = -\sigma_n - j\Omega_n$
- (c) $\psi_{a,n} = \psi_{a,n}^R + j\psi_{a,n}^I$

$$(d) \psi_{a,n}^* = \psi_{a,n}^R - j\psi_{a,n}^I$$

$$(e) \psi_{b,n} = \psi_{b,n}^R + j\psi_{b,n}^I$$

$$(f) \psi_{b,n}^* = \psi_{b,n}^R - j\psi_{b,n}^I$$

Resulting in:

$$H_{a,b}(S) = \sum_{n=1}^N \left[\frac{(\psi_{a,n}^R \psi_{b,n}^R - \psi_{a,n}^I \psi_{b,n}^I) + j(\psi_{a,n}^R \psi_{b,n}^I + \psi_{a,n}^I \psi_{b,n}^R)}{M_n(S + \sigma_n - j\Omega_n)} + \frac{(\psi_{a,n}^R \psi_{b,n}^R - \psi_{a,n}^I \psi_{b,n}^I) - j(\psi_{a,n}^R \psi_{b,n}^I + \psi_{a,n}^I \psi_{b,n}^R)}{M_n(S + \sigma_n + j\Omega_n)} \right] \quad (29)$$

This result may be simplified by placing the two terms of Eq. 29 over a common denominator as in Equation 30:

$$H_{a,b}(S) = 2 \sum_{n=1}^N \left[\frac{(\psi_{a,n}^R \psi_{b,n}^R - \psi_{a,n}^I \psi_{b,n}^I)(S + \sigma_n) - (\psi_{a,n}^R \psi_{b,n}^I + \psi_{a,n}^I \psi_{b,n}^R)\Omega_n}{M_n[(S + \sigma_n)^2 + \Omega_n^2]} \right] \quad (30)$$

Note that synthesizing an FRF from a complex-mode model only requires the $N \times N$ terms of the lower-left quarter of the modal transformation matrix given by Equation 22. For this reason, commercial modal analysis software does not retain the rest of the vector elements required in an analytic model. These additional terms are redundant; they may be constructed from the N roots and N vectors retained.

Normal Modes in a Complex-Mode Model

Clearly, real-mode solutions must be a subset of possible complex modes. But how are they represented in a complex-mode model? Comparing Equation 30 with 21 provides the answer. Equation 30 must collapse to 21 when a system's modes are solely normal. Expand the denominator of Eq. 30 and compare it to the denominator of Eq. 21:

$$M_n[(S + \sigma_n)^2 + \Omega_n^2] = M_n[S^2 + 2\sigma_n S + (\sigma_n^2 + \Omega_n^2)] \stackrel{?}{=} M_n(S^2 + 2\xi_n \omega_n S + \omega_n^2) \quad (31)$$

The two statements are identical if we define the *damping frequency* in radians/second:

$$\sigma_n = \xi_n \omega_n \quad (32)$$

and the *undamped natural frequency* in radians/second:

$$\omega_n^2 = \sigma_n^2 + \Omega_n^2 \quad (33a)$$

that is the *damped natural frequency* in radians/second is:

$$\Omega_n = \omega_n \sqrt{1 - \xi_n^2} \quad (33b)$$

Therefore, the denominator terms of the two summations are identical. Now compare the numerators:

$$\left[(\psi_{a,n}^R \psi_{b,n}^R - \psi_{a,n}^I \psi_{b,n}^I)(S + \sigma_n) - (\psi_{a,n}^R \psi_{b,n}^I + \psi_{a,n}^I \psi_{b,n}^R) \right] \stackrel{?}{=} \frac{\phi_{a,n} \phi_{b,n}}{2} \quad (34)$$

Equation 34 imposes two constraints on the complex mode formulation when real modes are the sole content. Equation 35a assures that there is no “ S proportional” term in the numerator, while Eq. 35b assures equality of the real-valued numerator:

$$\psi_{a,n}^R \psi_{b,n}^R - \psi_{a,n}^I \psi_{b,n}^I = 0 \quad (35a)$$

$$\psi_{a,n}^R \psi_{b,n}^R + \psi_{a,n}^I \psi_{b,n}^I = \frac{\phi_{a,n} \phi_{b,n}}{2\Omega_n} \quad (35b)$$

Since the vector elements of $\psi_{a,n}$ and $\psi_{b,n}$ must remain independent entities, these constraints are uniquely satisfied by Equations 36a and 36b.

$$\psi_{a,n}^R = -\psi_{a,n}^I = \frac{\phi_{a,n}}{2\sqrt{\Omega_n}} \quad (36a)$$

$$\psi_{b,n}^R = -\psi_{b,n}^I = \frac{\phi_{b,n}}{2\sqrt{\Omega_n}} \quad (36b)$$

This is a rather surprising conclusion. Intuition suggests that a real mode contained in a complex modal vector should exhibit the form: $\{k\phi_{i,n} + j0\}$. Instead, $\{k\phi_{i,n} - jk\phi_{i,n}\}$ is required. Therefore, a real-mode vector in a complex-mode model has elements with a -45° phase angle, not 0° .

Unusual Reality Check

I was introduced to the analog computer during my junior year in college; it was love at first sight. Professor Thomas Warner used an Electronic Associates TR-20 to light a fire in my soul. Several years later, with my first professional job astern, I came to work for Tom Harris in the Analog Computer facility of the Noise and Vibration Laboratory at General Motors Proving Ground. It was a wonderful experience in all ways. Harris and the analog computer became the trusted close friends of a lifetime. He taught me many things, perhaps the most important being that authoring a good analog simulation demonstrated mastery of a problem's underlying physics. Complex modes gave me a special problem in that regard – I could not conjure a circuit to model complex-mode behavior, nor could I find anyone else who had done so either. I searched diligently and dutifully for that circuit for many years, to no avail.

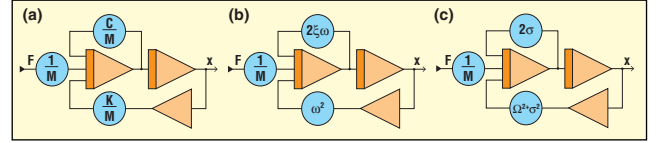


Figure 1. Analog computer simulation of base-constrained single-DOF spring, mass, damper system in terms of (a) physical impedance parameters, (b) undamped natural frequency and damping factor, (c) damped natural frequency and damping frequency.

Like anyone else who had ever used an analog computer, I could “patch” a three-amplifier lumped-mass, spring-mass-damper circuit quickly, be it an SDOF system such as that in Figure 1, or many lumps coupled in a variety of different ways. I was familiar with viewing such circuits in terms of physical parameters, undamped natural frequencies and damping factors or in terms of the system's roots or “poles” described by damped natural frequencies and damping frequencies. I had created patch panels describing structural dynamics in terms of test-measured, normal-mode parameters, including one that attempted to optimize a transmission tail-shaft vibration absorber for the then brand new Chevrolet Vega station wagon that suffered from terrible acoustic “boom periods.”

I never expected the analog computer to “map” a physical parameter circuit into a modal parameter circuit – those old beasts just didn't do that sort of task. What they did do, and quite brilliantly, was to let you “milk” a dynamic model with any “what if” question you could conjure. I simply wanted to patch a structure's description in terms of complex modes and play with it until I understood its behavior. Normal mode analogs were well understood but infrequently used. Complex modes were not intuitively understood, and no one claimed to have a complex-mode analog model one could study. I was long separated from the GM analog simulation lab when I accidentally stumbled on the circuit I had sought for so long. The first clue came from a cocktail-napkin error, with the damping strangely distributed across both integrators. This led to the normal-mode model of Figure 2. What was unique about the circuit was the fact that the coefficients of the dynamic loop were in terms of the damped natural frequency and the damping frequency, *separately*.

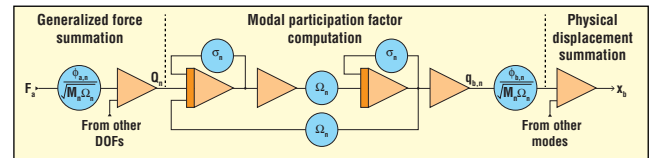


Figure 2. Symmetric analog of real-mode solution with damped natural frequency and damping frequency completely separated. Center circuit provides model's dynamics (Equation 18) for a single mode, while left and right summations implement Equations 19 and 20, respectively.

My epiphany moment came later when I realized the circuit of Figure 2 could be further generalized by adding another input and extracting a second output. Some painful algebra later, it was evident that an analog model could be cast in terms of complex-mode behavior. The circuit of Figure 3 was born, and my faith in complex modes was established.

The timing of that finding was fortuitous. As a vice president of Nicolet Scientific Corporation, I was leading that firm's effort to

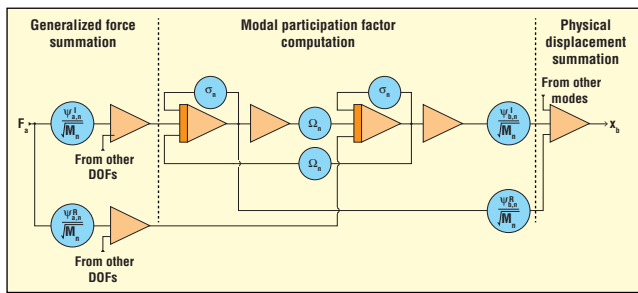


Figure 3. Adding second input to the inner loop allows it to solve complex-mode dynamics of Equation 25. Doubling the number of terms summed to form inputs and outputs completes generalized force summation of Equation 26 and modal participation transformation of Equation 27.

develop its first modal analysis system, the Model 6601. We were knee deep in curve-fitting algorithm development and badly needed “structures” with *known* real and complex modes to measure and analyze. An analog simulator proved to be the ideal answer. I designed the NSC Modal Simulator of Figure 4, incorporating the complex-mode circuit of Figure 3. We built this in about 1978, and it served the project well. Building a circuit that was controlled by the mathematics we were studying allowed us to interact with the mathematics in both cerebral and intuitive ways. Every member of the team gained new personal understanding of the complex-mode phenomena. This simulator was subsequently used in developing the Nicolet 6602 and 5885 modal systems as well as Schlumberger Technology’s Model 1202 modal analyzer before coming back into my possession.

Conclusions

We have reviewed the classical derivation of normal modes and complex modes from a series of second-order ordinary differential equations with constant coefficients written in matrix notation. Further, we have examined the synthesis of frequency response functions, such as those used in curve-fitting measurements made in experimental modal analysis. These studies make clear the redundancies contained in a complex-mode model. The matrices that state the complex-mode problem contains solely *real* values. However, describing an N mode by N degree-of-freedom problem requires matrices of $2N \times 2N$ dimension, quadrupling the number of problem coefficients. The solution provides $2N$ modes, each including a modal vector of length $2N$ populated by *complex* elements. However, half the modes are redundant, being the conjugates of N unique modes found. Within the unique modal vectors, half of the elements are redundant; being the unique displacement shape coefficients multiplied by the eigenvector’s associated *complex* eigenvalue or pole.

Commercial systems performing experimental modal analysis only retain one quarter of the complex-mode coefficients found in an analytic modal analysis. The N modes retained are all unique; there are no matching conjugates. The retained complex eigenvector elements are solely the system’s N modal displacements; the N modal velocities are not included in these vectors. It was




Figure 4. Analog modal simulator built for internal research at Nicolet Scientific Corp. in the late 1970s. Each mode was programmed by soldering selected precision resistors in place. Programming “rules” were printed on the component side of a two-layer PC. Card on left holds a real-mode shape; one on right defines complex mode. Each card contained coefficients for 5 degrees of freedom. Simulated frequency response function could contain as many modes as there were cards plugged into frame. BNCs and rotary switches at left allowed simultaneous excitation up to three DOFs and simultaneous displacement measurement at same or three other DOFs. Results were analyzed using the Nicolet 660 series FFT analyzer, a highly capable two-channel instrument.

demonstrated through comparison of FRF synthesis that both experimental and analytic models contain exactly the same information. An interesting fallout of this comparison is the format of real-mode vectors in a complex-mode model. The vectors in this case are *complex valued*, of the form $\{k\phi_{i,n} - jk\phi_{i,n}\}$, exhibiting -45° phase at every element.

The authors of Reference 1 first conceived the complex-mode formulation of Equation 11. They were also the originators of matrix iteration. Both of these matters are more clearly described in Reference 2. Reference 3 first disclosed the proper form of real-mode vectors contained in a complex-mode model, while Reference 4 explains why a complex-mode model may be superior for predicting the effects of structural modifications. The analog circuit of Figure 3 was first described in Reference 5. Reference 6 provides a brief but solid introduction to analog computational methods.

Bibliography

1. Frazier, R. A., Duncan, W. J., Collar, A. R., *Elementary Matrices*, Cambridge: At The University Press, 1950.
2. Hurty, W. C., Rubinstein, M. F., *Dynamics of Structures*, Prentice-Hall, Inc., 1964.
3. Lang, G. F., “Modal Testing Principles,” Technical Report Number 023/87, Schlumberger, 1987.
4. Lang, G. F., “Demystifying Complex Modes,” *Sound & Vibration*, January 1989.
5. Flannelly, W. G., Lang, G. F., “Modal Analysis for Managers”, *Sound & Vibration*, November 1979.
6. Lang, G. F., “Analog was *Not* a Computer Trademark,” *Sound & Vibration*, August 2000. 

The author can be reached at: george@langslair.com.